The heating sensor PIR detector by radiation and its computer simulation.

R. Drga, D. Janáčová, H. Charvátová, V. Vašek

Abstract— In the security industry is the most commonly used PIR detector. At its behaviour is focused in this work. It was necessary to design a mathematical model of heat sensor simulation and thermal behaviour of the sensor in COMSOL Multiphysics environment followed by verification of the proposed mathematical model. Theoretical and mathematical conclusions became the basis for the subsequent implementation of workplace IR radiation for measuring the properties of radiation sources and sensors, in particular spatial characteristics PIR detectors..

Keywords— radiation, pyroelement, mathematical model, PIR detector.

I. Introduction

THIS work deals with the use of infrared radiation in the security industry and solves the problem of testing detectors, security systems, where it is relatively difficult to verify their properties. A special area represent PIR detectors, because their design does not allow direct measurement of the sensor and proprietary radiation from an intruder passes through the optical system, which is in the form of Fresnel lenses, or use a mirror surface.

The results of this work can be also used in technical subjects means security industry, electronic security systems, which are the subject of teaching at the Institute of Security Engineering Faculty of Applied Informatics Tomas Bata University in Zlin. The work is focused primarily on PIR detectors, which are used most widely in security technologies. For thermal balance PIR detector and pyroelement was necessary to propose a mathematical model described below, perform simulations of the thermal behaviour of the sensors in the environment, COMSOL Multiphysics and verify the accuracy of the measurement pyroelement time close to zero at low density thermal radiation.

The work was performed with financial support of research project NPU I No. MSMT-7778/2014 by the Ministry of Education of the Czech Republic and also by the European Regional Development Fund under the Project CEBIA-Tech No. CZ.1.05/2.1.00/03.0089.

Rudolf Drga, Tomas Bata University in Zlín, Faculty of Applied Informatics, Department of Security Engineering, Nad Stráněmi 4511, 760 05 Zlín , Czech Republic (e-mail: rdrga@fai.utb.cz).

Dagmar Janáčová, Tomas Bata University in Zlín, Faculty of Applied Informatics, Department of Automation and Control Engineering, Nad Stráněmi 4511, 760 05 Zlín , Czech Republic (e-mail: Janáčová@fai.utb.cz).

Hana Charvátová, Tomas Bata University in Zlín, Faculty of Applied Informatics, Regional Research Centre CEBIA-Tech, Nad Stráněmi 4511, 760 05 Zlín , Czech Republic (e-mail: Charvátová@fai.utb.cz).

Vladimír Vašek, Tomas Bata University in Zlín, Faculty of Applied Informatics, Department of Automation and Control Engineering, Nad Stráněmi 4511, 760 05 Zlín , Czech Republic (e-mail: vasek@fai.utb.cz).

II. Mathematical model of heating sensor by radiation

Thermal radiation incident on the sensor is partially reflected and some is absorbed by the sensor, thereby to ensure that the temperature measured at the beginning of the measurement does not fully effective temperature.

For the quantitative description of the temperature distribution in the heated pyroelement radiation we used the Stefan-Boltzmann law, according to which the density of heat flow between the source and the heated surface expressed as (1) [3]:

$$q(\tau) = \sigma.C(T_2^4 - T_1^4) \tag{1}$$

where: σ - Stefan-Boltzmann constant
C - emission surface and geometric properties, [1]
T_2 – source temperature, [K]
T_1 – temperature of heated surface, in this case the surface temperature, [K]

$$\frac{\partial T}{\partial \tau} = a.\frac{\partial^2 T}{\partial x^2}\ ;\ 0 < x < b, 0 < \tau \tag{2}$$

$$W_1 = konst \cdot T_1^5\ . \tag{3}$$

$$\lambda\left(\frac{\partial T}{\partial x}\right)_{x=b} = q\ . \tag{4}$$

$$T = T_p \quad \text{for} \quad \tau = 0 \tag{5}$$

where:
b - half the thickness of the sensor, [m]
x - direction coordinates, [m]

Laplace transform of equation (1) with conditions (2) to (5) has been obtained analytical solution of unsteady temperature field for symmetrically heated by radiation sensor plate shape:

$$\frac{T-T_p}{T_c-T_p}=K_i\left[Fo+\frac{1}{2}\left(\frac{x}{b}\right)^2-\frac{1}{6}-2\sum_{n=1}^{\infty}\frac{\cos\left(\frac{x}{b}p_n\right)}{p_n{}^2\cos\ p_n}e^{\left(-Fop_n{}^2\right)}\right]. \qquad (6)$$

where Ki is Kirpičev criterion (7)

$$\lambda\left(\frac{\partial T}{\partial x}\right)_{x=b}=q\,. \qquad (7)$$

where T_c is medium temperature of radiators.
Fourier criterion *Fo* represents the dimensionless heating time is calculated by the equation:

$$Fo=\frac{a\tau}{b^2} \qquad (8)$$

where:
τ - duration of heating, [s]
a - thermal conductivity sensor, [$m^2.s^{-1}$]:

$$a=\frac{\lambda}{\rho c_p} \qquad (9)$$

where:
λ - the thermal conductivity sensor, [$W.m^{-1}.K^{-1}$]
ρ - the density of the sensor material, [$kg.m^{-3}$]
c_p - the specific heat capacity of the sensor material, [$J.kg^{-1}.K^{-1}$].

Members *p* of the analytical solution of (6) are determined from equation (10):

$$p_n=n\cdot\pi \qquad (10)$$

According to the form the solution (6) it is evident that with increasing time of heating effect element endless series decreases, i.e., we can also expect Fourier criterion *Fo* which influence endless series may be neglected and *Fo* > *Fok* the temperature at any point in the wall almost linear function time and temperature profile across the plate (x-axis direction) is a parabola.

III. Solution of a Mathematical Model in the Maple Environment

Solution temperature distribution in pyroelement according to equation (6) was performed using the software applications created in Maple environment. To this purpose, the program created an application that performs automatic calculation of temperature fields for the specified input value. The source code is as follows:

Defining input values:

```
> q:=1;
> b:=0.005;
> lambda:=4.6;
> tc:=36;
> tp:=20;
> rho1:=7450;
> cp:=250;
> a:=lambda/(rho1*cp);
> Fo:=a*tau/b^2;
```

The calculation of the roots of p:

```
> for i from 1 to 300 do
p[i]:=evalf(Pi*i)
end do;
```

$p_1 := 3.141592654$
$p_2 := 6.283185308$
$p_3 := 9.424777962$
⋮

Calculation of 3D temperature field based on the analytical solution (6):

```
> with(plots):
>grafreal:=plot3d((q/lambda*(a*tau/b+x^2/(2*b)-(b/6))-2*q*b/lambda*Sum(cos(x/b*p[n])*exp(-(a*tau/b^2)*p[n]^2)/(p[n]^2*cos(p[n])),n=1..300))+tp,x=0..b,tau=0..60,axes=box,style=wireframe,color=red ,labels=["x (m)","tau (s)","t (degC)"]):
> display(grafreal);
```

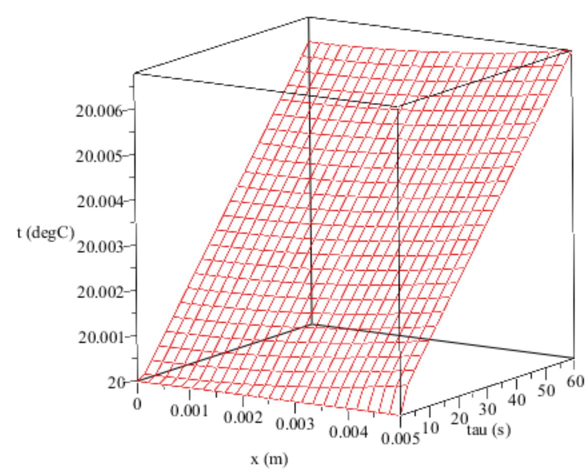

Fig. 1 3D temperature field in a heated sensor calculated in Maple

Calculation of temperature fields in 2D on the basis of analytical solutions (6):

```
> for j from 1 to 10 do
fce2D[j]:=q/lambda*(a*tau[j]/b+x^2/(2*b)-(b/6))-
2*b/lambda*Sum(cos(x/b*p[n])*exp(-
(a*tau[j]/b^2)*p[n]^2)/(p[n]^2*cos(p[n])),n=1..300)+tp
end do:
> for k from 1 to 10 do
tau[k]:=6*k
end do;
```

$\tau_1 := 6$

$\tau_2 := 12$

$\tau_3 := 18$

$\vdots$

```
>graf1:=plot(fce2D[1],x=0..b,legend=tau[1],axes=box,color=
COLOR(HUE, .1)):

>graf2:=plot(fce2D[2],x=0..b,legend=tau[2],axes=box,color=
COLOR(HUE, .2)):

>graf3:=plot(fce2D[3],x=0..b,legend=tau[3],axes=box,color=
COLOR(HUE, .3)):
⋮

>display(graf1,graf2,graf3,graf4,graf5,graf6,graf7,graf8,graf9,
graf10);
```

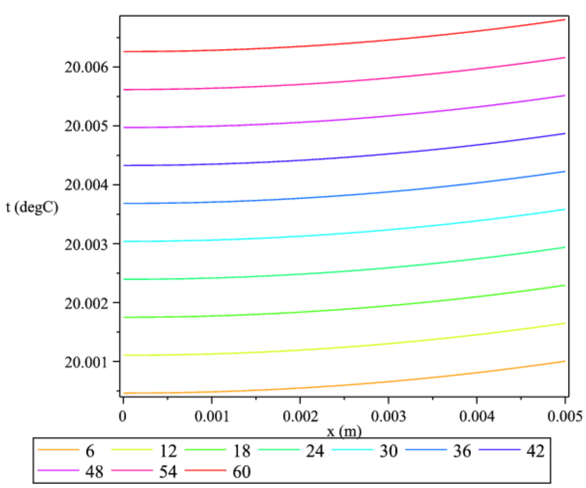

Fig. 2 2D temperature field in a heated sensor calculated in Maple

Calculation of the temperature sensor in the desired location and time:

```
> x[zvol]:=0.002;
```

$x_{zvol} := 0.002$

```
> tau[zvol]:=550;
```

$\tau_{zvol} := 550$

```
>evalf((q/lambda*(a*tau[zvol]/b+x[zvol]^2/(2*b)-(b/6))-
2*b/lambda*Sum(cos(x[zvol]/b*p[n])*exp(-
(a*tau[zvol]/b^2)*p[n]^2)/(p[n]^2*cos(p[n])),n=1..300)+tp)
);
```

20.05898920

The output of the program application is a plot showing the 3D and 2D real temperature field in a heated sensor to the desired input value. 3D temperature field shows the temperature distribution for a selected period of heating sensor (Fig. 1). 2D temperature field shows the temperature curve of the sensor at the desired times of heating (Fig. 2). The application also calculates the temperature of sensor in a given place and time, as shown in the last part of the above source file.

IV. Simulation and Verification Proposed Models in COMSOL Multiphysics

Because it was not possible to determine experimentally the necessary data, was used to assess the thermal behavior of the sensor software COMSOL Multiphysics, which is suitable for the simulation of physical processes and is intended primarily for developers, researchers and researchers.

The aim of simulation is to determine the temperature distribution and the heat flow density in the surface of the pyroelectric element location depending on the distance from the intruder detector. The "Heat Transfer Module" was used for the simulation, for environment "Surphace-to-Surphace Radiation". Size intruder simulating the glowing area of 2 m x 0.5 m, the properties of the detector represents pyroelement of size 5 mm x 2.3 mm x 0.2 mm. The simulation was performed under the conditions:

the surface temperature of an intruder 36 °C

ambient air temperature 20 °C

relative emissivity of the surface of a pyroelectric element 0.9

relative emissivity of 0.97 intruder

thermal conductivity of the pyroelectric element 2,255.10-6 m2/s

thermal conductivity intruder 1,484.10-7 m2/s

thermal conductivity of air 2,14.10-5 m2/s

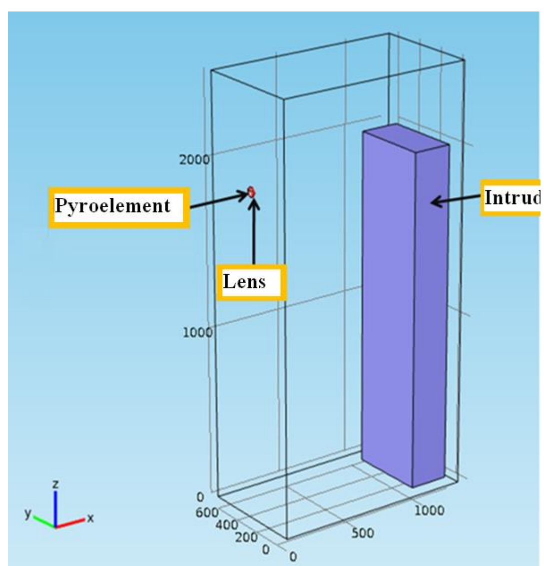

Fig. 3 The geometric layout of the situation

The following figures show the results of simulation, ie, the distribution of temperature and heat flux density on the surface of a pyroelectric element distance from the intruder detector from 1m to 5m.

Fig. 4, 5, 6, 7 are simulation results for a distance of 1 m from the detector to intruder. Fig. 4 shows a section showing the distribution of temperature at the surface pyroelementu for intruder detector distance from 1 m. On Fig. 5 is displayed then detail the temperature distribution in the vicinity of pyroelementu. It is obvious that in the vicinity pyroelementu there is an increase in air temperature due to the temperature at a greater distance from the detector. The Fig. 6. shows the density distribution of the heat flow in the cross-sectional surface at the point pyroelementu, the Fig 7. picture is then detail the distribution of heat flux density in the vicinity pyroelementu. Near pyroelementu heat flux density increases until it reaches a value of approximately 0.5 W / m 2 due to the higher relative to the surroundings..

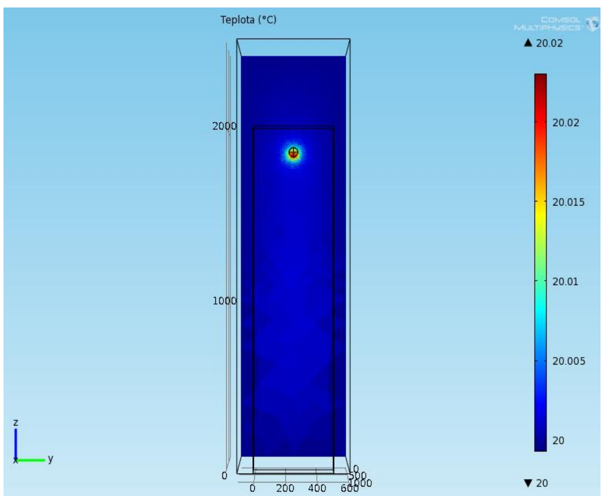

Fig. 4 The temperature distribution in the cross-sectional surface at the site of a pyroelectric element for 1 m

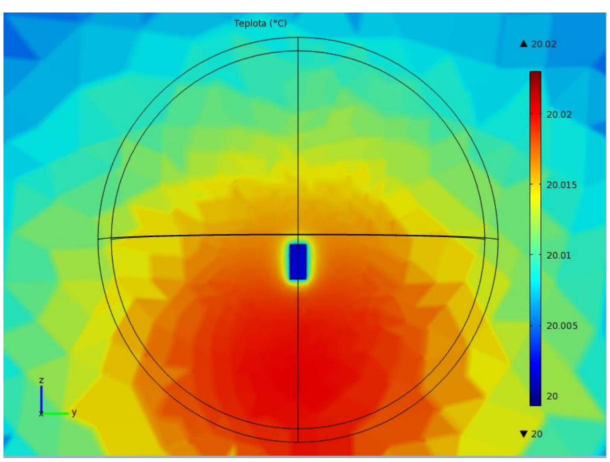

Fig. 5 The temperature distribution in the cut surface at the point a pyroelectric element - detail in location of the detector

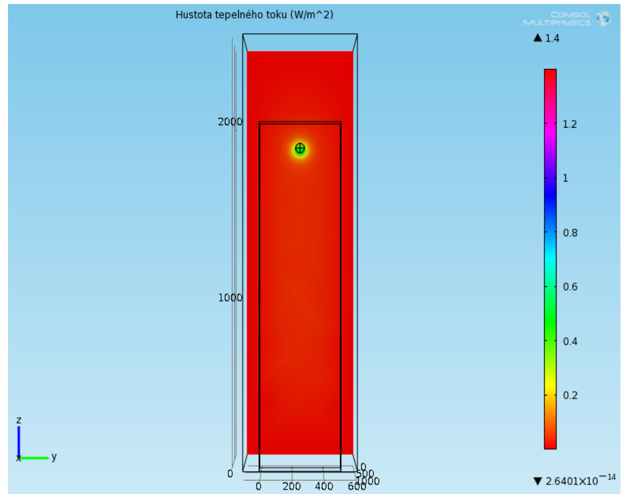

Fig. 6 The temperature distribution in the cut surface at the site of a pyroelektric element - detail the location of the detector

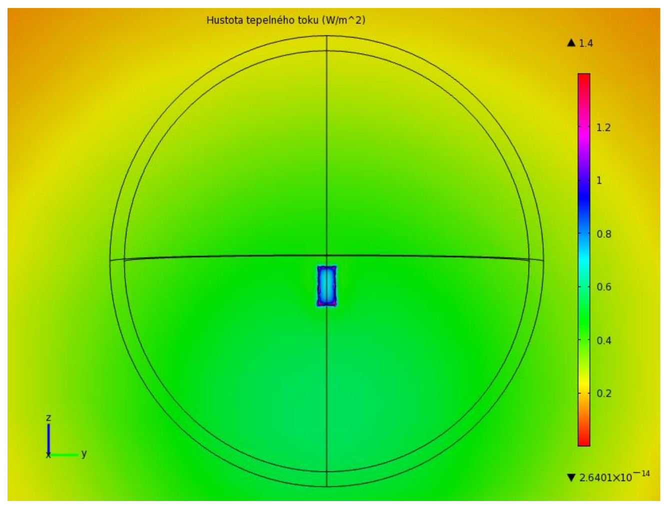

Fig. 7 The distribution density of the heat flow at the site of the cut surface of the pyroelectric element - detail in the place of the detector

Fig. 8, 9, 10, 11 are simulation results for a distance of 3 m from the detector to intruder.

In this case decreased heat flux density to a value of about 0.24 W / m 2 and also further decrease of the surface temperature pyroelementu, as shown on Fig. 11^{th}.

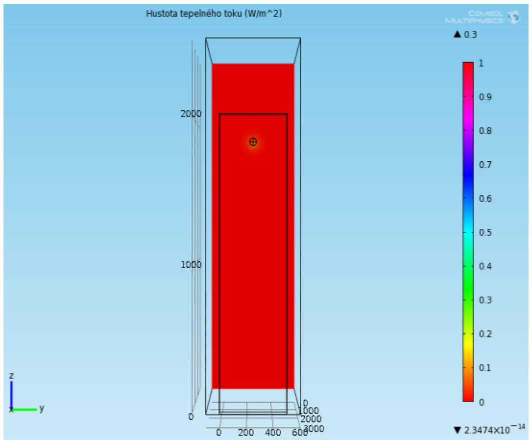

Fig. 8 The temperature distribution in the cross-sectional surface at the site of a pyroelectric element

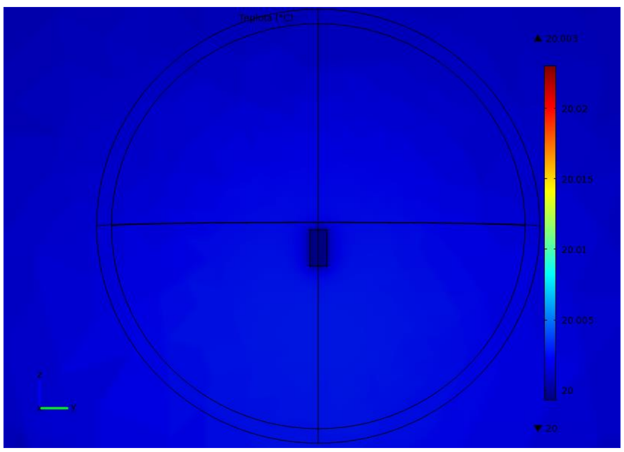

Fig. 9 The temperature distribution in the cut surface at the point a pyroelectric element - detail in location of the detector

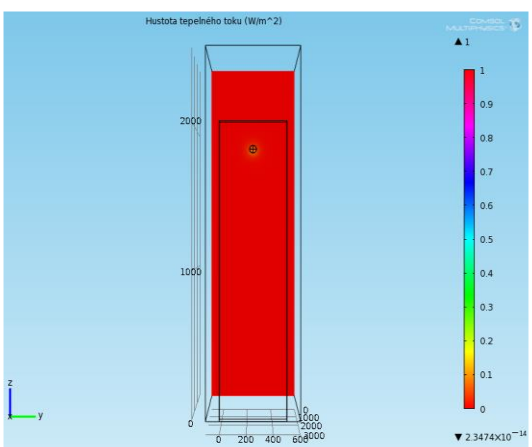

Fig. 10 The temperature distribution in the cut surface at the site of a pyroelektric element - detail the location of the detector

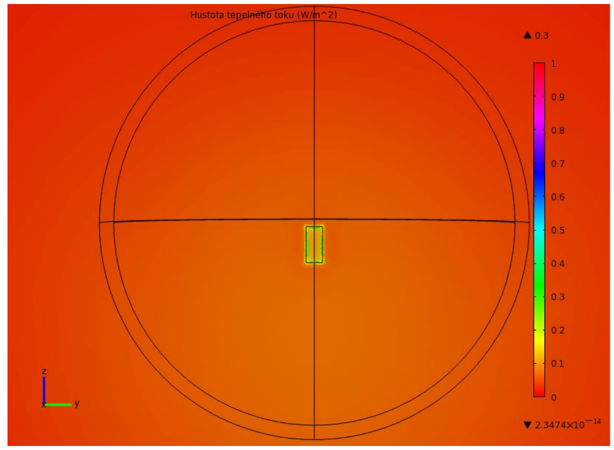

Fig. 11 The distribution density of the heat flow at the site of the cut surface of the pyroelectric element - detail in the place of the detector

In the case of an intruder detector distance 3 m decreased heat flow density to approximately 0.24W/m2, while a further decrease of the surface temperature pyroelement.

Fig. 12, 13, 14, 15 are simulation results for a distance of 5 m between the detector and intruder.

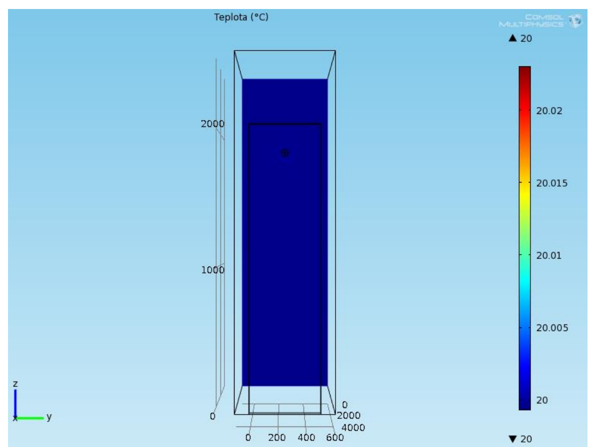

Fig. 12 The temperature distribution in the cross-sectional surface at the site of a pyroelectric element

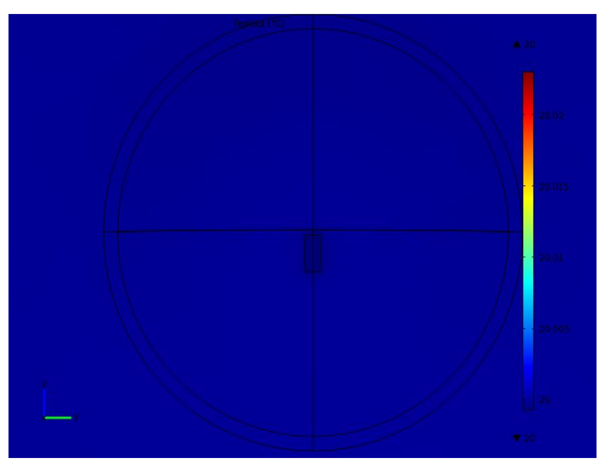

Fig. 13 The temperature distribution in the cut surface at the point a pyroelectric element - detail in location of the detector

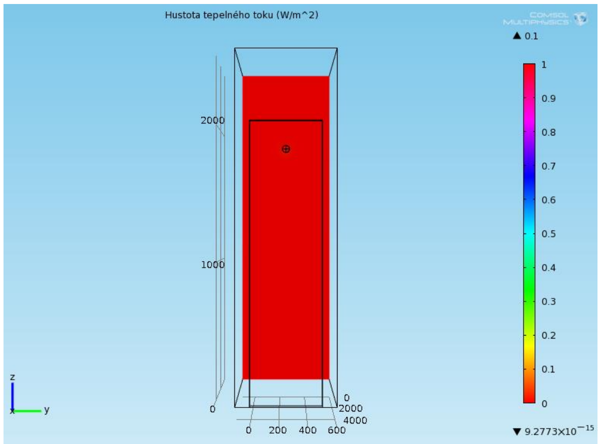

Fig. 14 The temperature distribution in the cut surface at the site of a pyroelektric element - detail the location of the detector

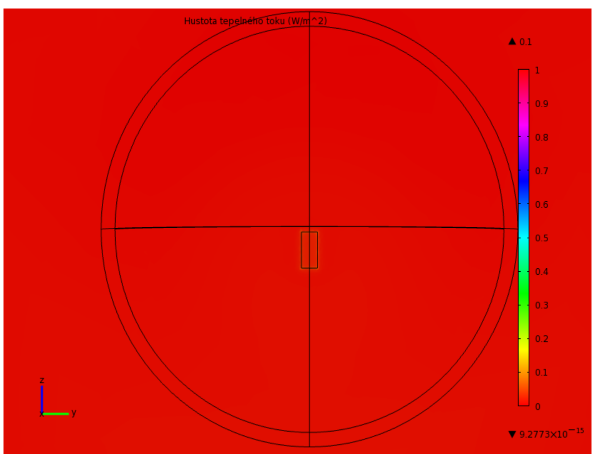

Fig. 15 The distribution density of the heat flow at the site of the cut surface of the pyroelectric element - detail in the place of the detector

Specified the value of the density of heat flow and temperature at the surface pyroelement according to the results of simulation in COMSOL Multiphysics is detailed in the following table. These values correspond to the mid-position of the element.

Table I Heat flux density on the surface of the pyroelectric element - the results of simulation in COMSOL Multiphysics

Distance of detector from intruder [m]	Heat flow density [W/m²]	Heat flow density [W/m²]
1	0,750	20,0230
2	0,380	20,0076
3	0,245	20,0012
4	0,035	20,0010
5	0,020	20,0004

The table shows that with increasing distance decreases heat flow density on the surface of the original pyroelement 0.75 W/m2 at 0.02 W/m2. It also reduces the surface temperature pyroelement value of 20.023 °C at 20.0004 °C.

V. Calculation of Temperature Fields in Maple

The density of heat flow, obtained by simulation in COMSOL Multiphysics is used for the calculation of unsteady temperature fields in pyroelement according to the analytical solution (6) model (2) - (5). For the calculation of temperature fields were used the following values:
element thickness 0.2 mm
initial temperature of the pyroelectric element 20 ° C
surface temperature of the intruder (source) 36 °C
The following pictures show waveforms of temperature on the surface pyroelement in terms of heat flow density from 0.75 W/m2 to 0.02 W/m2, which corresponds to the distance from the intruder detector 1 m to 5 m.

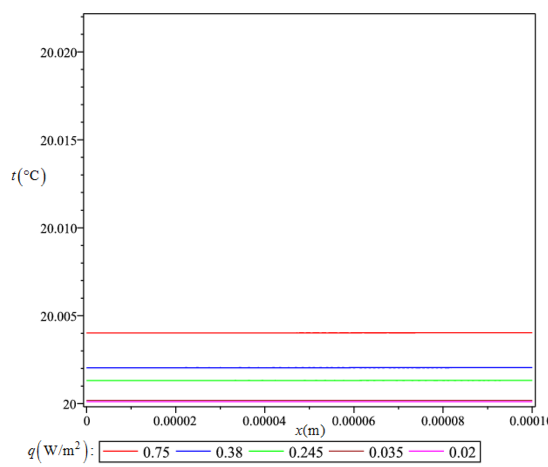

Fig. 16 The duration of heat exposure: 1 second

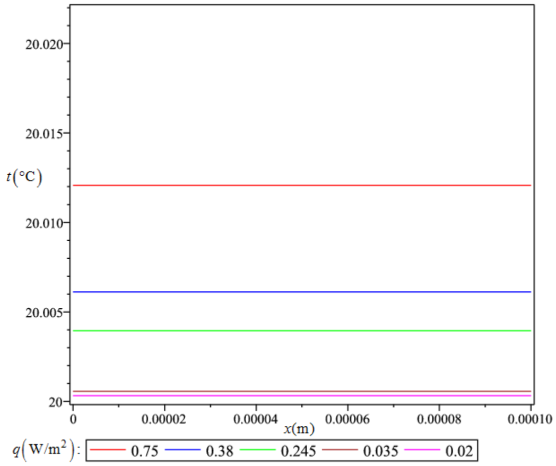

Fig. 17 The duration of heat exposure: 3 seconds

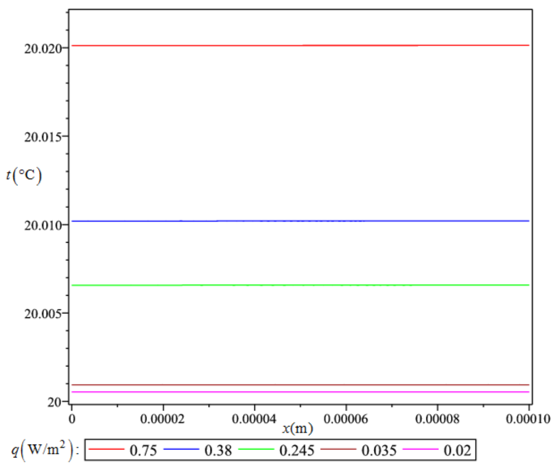

Fig. 18 The duration of heat exposure: 5 second

From the graphs it is evident that the heat treatment for 1-5 seconds for incident radiation having a density of 0.75 W/m^2 temperature pyroelement increased about 0.015 °C, while for incident radiation having a density of 0.02 W/m^2, the temperature hardly increased pyroelement.
The calculations and simulations, the temperature distribution in the heated pyroelement also shows that even at low values of the density of heat flux at a given time, the surface temperature pyroelement nearly the same temperature throughout its thickness (no steep temperature field). This proves that pyroelement is flawed. It can be said that in the early stages of measurement evaluates pyroelement right temperature and laboratory measurements is therefore in the initial stages sufficiently accurate

VI. Comparison of Theoretical Results with Simulations

Verification of the mathematical model was made by comparing the temperature fields in pyroelement calculated in the Maple on the basis of the analytical solution described by equation (6) with the results of the simulation of temperature field in COMSOL Multiphysics.

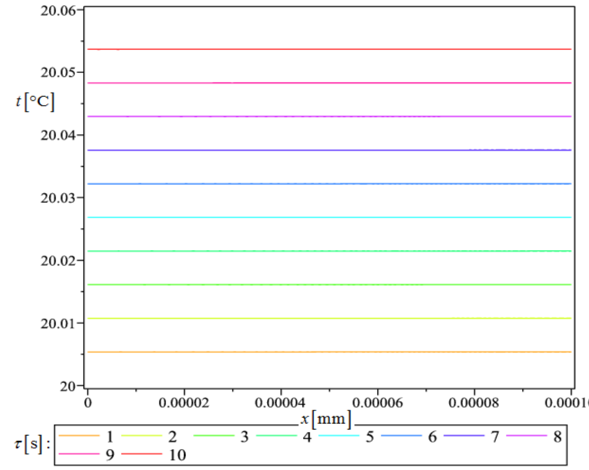

Fig. 19 Temperature field in pyroelement for the heat of the action 10 seconds calculated in Maple

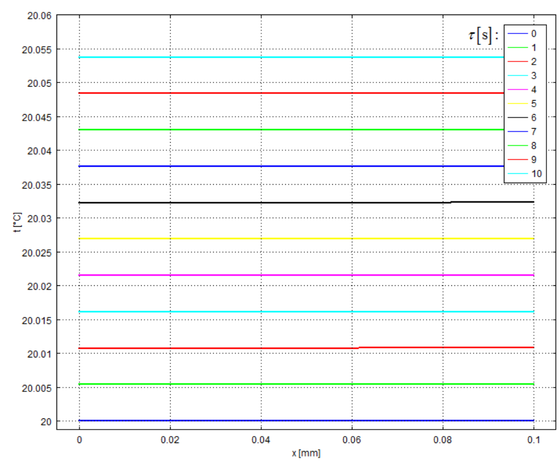

Fig. 20 Temperature field in pyroelement for the heat of the action 10 seconds calculated in COMSOL Multiphysics

It is evident that the curves of temperature fields calculated in Maple coincide with the courses of temperature fields obtained by simulation in COMSOL Multiphysics.

VII. Conclusion

Analytical solution of the proposed mathematical model describing heat radiation sensor was used to create applications for the calculation of temperature fields in pyroelement in the user interface of the program Maple. Because it was not possible to determine all the data needed for the calculation of temperature field experimentation was conducted simulations to assess the thermal behavior pyroelement programming environment COMSOL Multiphysics. The simulations were designed waveforms temperature fields and heat flux density at the surface and under surface pyroelement for the selected distance from the intruder detector. The data obtained were then compared with the theoretical results obtained by the solution of the model through an application program created in Maple environment.

The calculations and simulations, the temperature distribution in the heated pyroelement showed that even at low values of heat flow density in a given time the surface temperature pyroelement nearly the same temperature throughout its thickness, which confirmed that in the early stages of measurement evaluates pyroelement right temperature and laboratory measurements is therefore in the initial stages is sufficiently accurate.

Based on the theoretical results and the mathematical description was later realized laboratory workplace interior IR radiation, which was made specific measurements of the properties of radiation sources and detectors , and where it is also possible to measure the spatial characteristics PIR detectors.

REFERENCES

[1] Vincent, J., D. *Fundamentals of infrared detector operation and testing*. USA – Texas. WILEY, 1990

[2] Knoll G., F. Radiation detection and *measurement*. USA – Texas: WILEY, 2000

[3] Saleh B., E., A., Teich, M. C. *Fundamentals of photonics*. USA – Texas: WILEY, 2007

[4] Kolomazník, K. *Teorie technologických procesů III*. (in Czech). University of Technology in Brno, Brno, 1978

[5] JHA, A., R. *Infrared technology*. USA – Texas: WILEY, 2006

[6] Hotz C. Hottel, Adel F. Sarofim. *Přenos tepla zářením*. (in Czech). SNTL Praha, 1979.

[7] Kolomazník, K. *Modelování zpracovatelských procesů* (in Czech), Brno:Vysoké učení technické v Brně, 1990.

[8] Židek, K., Piteľ, J. *Smart 3D Pointing Device Based on MEMS Sensor and Bluetooth Low Energy*. In: Proceedings of the 2013 IEEE Symposium on Computational Intelligence in Control and Automation (CICA), Singapore, April 16-19, 2013. Singapore: IEEE, 2013. pp. 165-168. ISBN 978-1-4673-5847-7.

[9] Makovník, R., Líška, O. *Contribution to experimental identification and simulation problems of dynamic systems*, In: Ovidius University Annual Scientific Journal. Vol. 9, No. 1, p. 28-32, 2007, ISSN 1224-1776

[10] Líška, O. *Monitorizačné systémy pre automatiozvanú výrobu* (in Slovak), In: Transfer inovácií. Č. 12 (2008), s. 121-123. - ISSN 1337-7094, 2008, Available from: http://www.sjf.tuke.sk/

[11] M. Fodor, O. Líška *Design and realization sensorial system on detection obstacle* / - 2010. - 1 elektronický optický disk (CD-ROM).In: SAMI 2010 : 8th International Symposium on Applied Machine Intelligence and Informatics : January 28-30, 2010, Herľany, Slovakia. - [s.l.] : IEEE, 2010 S. 243-245. - ISBN 978-1-4244-6423-4 Available from: http://www.sami.tuke.sk.

Rudolf Drga is an Associate Professor in the Department of Security engineering, Faculty of Applied Informatics of Tomas Bata University in Zlín. His research activities include electronic security systems.

Dagmar Janáčová is a Professor in the Department of Automation and Control Engineering, Faculty of Applied Informatics, Tomas Bata University in Zlín. Her research activities include: modeling of treatment processes of natural polymers, transport processes, recycling of tannery waste, optimization and ecological approach of tannery processes.

Vladimír Vašek is a Professor in the Department of Automation and Control Engineering, Faculty of Applied Informatics, Tomas Bata University in Zlín. His research activities include: microcomputer applications in technology processes, computer monitoring and control systems, discrete deterministic controllers approach of tannery processes.

Hana Charvátová is a research worker in the Regional Research Centre CEBIA-Tech, Faculty of Applied Informatics, Tomas Bata University in Zlín. Her research activities include recycling technology, transport processes and mathematical modeling of natural and synthetic polymers treatment.